- Technical Paper -

STRENGTH OF RC BEAM-COLUMN JOINT IN SOFT-FIRST STORY WHERE FIRST-STORY COLUMNS ARE EXTENDED OUTSIDE

Sefatullah HALIM[*1], Susumu TAKAHASHI[*2], Toshikatsu INCHINOSE[*3] and Masaomi TESHIGAWARA[*4]

ABSTRACT

Strut-and-tie models were developed for beam-column joint in soft-first story where first-story columns were extended toward outside. The developed models agreed with the observed crack patterns. The developed models were different from those for knee joints in that large struts were extended into the second-story column and the wall panel. Based on the strut-and-tie models new design equations were proposed, where the joint strength is evaluated as the sum of the flexural strengths of the beam and the second-story column.

Keywords: beam-column joint, strut-and-tie model, soft-first story, knee joint

1. INTRODUCTION

In the design of a single-bay apartment building with a parking lot in the first story (Fig. 1a), a designer may extend the column depths in the first story toward outside due to architectural designs and expecting larger strength and stiffness.

The designer may consider the beam-column joint as a usual knee joint looking to its geometry and anchorage of bars. There are many researches on knee joints, e.g. Shiohara and Shin [1]. However, the existence of the second story (Fig. 1a) makes the problem different. Also, this case may look similar to a pile cap connecting cast-in-place pile, foundation beam, and first story column, because the ratio of the diameter of such a pile to the depth of first story column is comparable with that of the depths of the columns shown in Fig. 1a. There are some researches on pile cap, e.g. Iizuka et al [2]. However, the existence of the wall panel in the second story (Fig. 1a) makes the problem different.

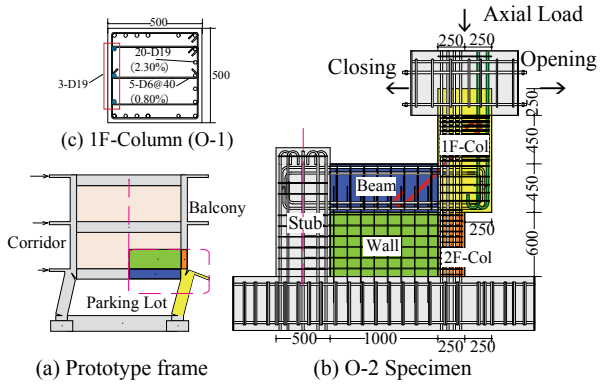

Fig.1 Elevation view of frame and specimen

In this paper, strut-and-tie models (STMs) are developed for such joints. STMs are also developed for usual knee joint to understand the effects of the wall panel on the joint strength. Based on the STMs new design equations to compute the strength of such joints are proposed considering the effects of boundary beam and column.

2. TEST PROGRAM AND RESULTS [3]

Kotani, et al [3] tested specimens depicting beam-column joints denoted by the dashed pink line in Fig. 1a. In the prototype building, the depths of the columns in the first story were assumed twice of those in the upper stories (Fig. 1a). A large boundary beam was assumed at the bottom of the wall to reduce the probability of joint failure shown in Fig. 1a. The specimens were constructed upside down to easily apply the loads as shown in Fig. 1b with the scale of one-half. The vertical stub in Fig. 1b is constructed to represent the remaining part of the frame in Fig. 1a, which is supposed to have negligibly small deformation under the applied loads. The upper stub is located at the loading point, which represents mid-height of the first story.

The test parameter was the difference of reinforcement such as inclined bars shown by the red line in Fig. 1b. Longitudinal reinforcements in the outermost two layers of first story column (9-D19, green in Fig. 1b) were anchored with 180 degree hook at the joint while the remaining bars passed into second story column (Fig. 1b).

Displacement was controlled at the loading point. Axial force equal to 30% (2250kN) of first story column capacity was applied in the closing direction

*1 Graduate Student, Nagoya Institute of Technology, JCI Student Member
*2 Assistant Prof., Dept. of Architecture, Nagoya Institute of Technology, JCI member
*3 Prof., Dept. of Architecture, Nagoya Institute of Technology, JCI member
*4 Prof., Dept. of Environmental Engineering and Architecture, Nagoya University, JCI member

and no axial load was applied in the opening direction considering overturning mechanism of the structure.

In this paper, two specimens are discussed: O-1 with the first-story-column section shown in Fig. 1c and O-2 with the inclined reinforcement (5-D19) shown in red in Fig. 1b. In O-2 specimen, 3-D19 bars indicated by the red rectangle in Fig. 1c were not provided so that the flexural strength of first story column of the two specimens would be the same. The red and green lines in Fig. 2 show the envelopes of the observed load-deformation relationships. The blue lines show analytical lateral strength based on flexural capacity of first story column at the beam bottom face. The strength is computed using Bernoulli-Euler assumption, so strain is distributed linearly in the section. Hognestad model [4] is used for concrete stress-strain relationship and bi-linear model is used for steel. The strengths of the two specimens observed in the opening (positive) load were less than 2/3 of the computed ones. The strength of O-1 specimen observed in closing (negative) load was almost equal to the analytical strength in this direction. The strength of O-2 specimen observed in closing (negative) load was smaller than analytical strength. The inclined bars of O-2 specimen (red in Fig. 1b) did not yield in compression. The inclined bars were detrimental and failed to transfer the compressive force to the second story.

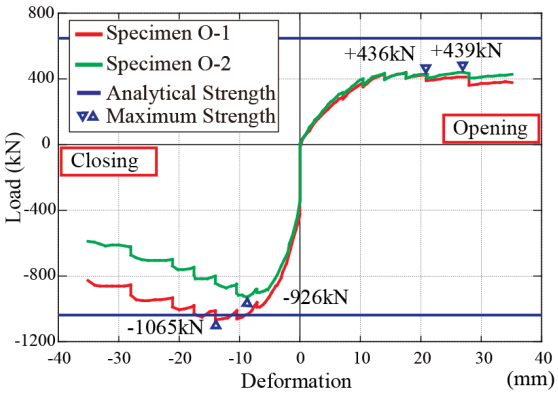

Fig.2 Load-Displacement relationship

3. STRUT-AND-TIE MODELS FOR SPECIMENS

Strut-and-tie models (STMs) are developed for specimens to understand the flow of internal forces and probable failure mechanisms.

Figures 3 and 4 show the developed strut-and-tie models for opening load of O-1 and O-2 specimens, respectively. Blue lines show bars in tension. Solid blue lines indicate tensile yielding while dashed lines indicate below yield.

Strut-and-tie models for the opening direction were determined assuming as follow:

(1) Moment by the forces acting on the stub is zero around node A.

(2) The three layers of the column main bars (AE in Figs. 3) resist tension. The beam bottom bars, the inclined bars, vertical bars in wall panel and the stirrups also resist tension.

(3) Effective compression strength of concrete to determine strut's width is assumed to be 85% of concrete strength.

The strut width is determined as follow:

$$W_{strut} = \frac{C_{strut}}{(0.85 \times f_c' \times b)} \quad (1)$$

where, C_{strut} is compression force of a strut, f_c' is concrete strength and b is width of each element that strut goes through. Because the thickness of the wall panel was 100 mm and 1/4 of the width of the beam (400mm), the width of each strut widens by 4 times at the boundary of the beam and the wall panel. Similar changes occur at the boundary of the beam and the column, too.

(4) Node B is located at centerline of the beam bottom bars such that the outer edge of the nodal zone coincides with the outermost point of hooked beam bottom bars (see Fig. 4).

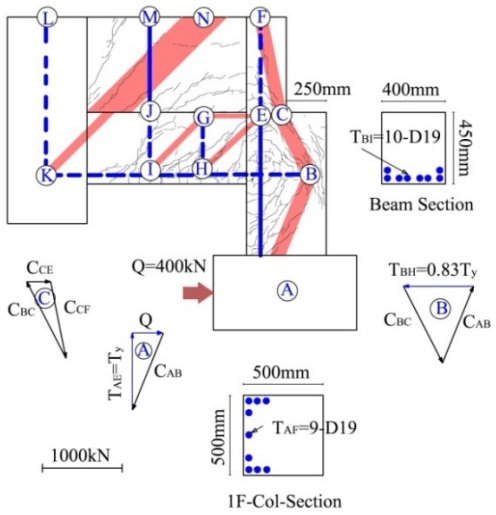

Fig.3 Strut and tie model of O-1(Opening)

Optimization is carried out to find a model with maximum strength. At first, force in the tie AE is considered equal to the yield strength of the first story column tensile bars. Later on forces in all struts and ties are computed. Shear reinforcement in the first story column is not shown as they have big shear capacities relative to the opening load, but are shown in case of closing load which will discuss later (Figs. 5 and 6). The joint hoops are much smaller than the beam, thus, its effects on lateral strength are neglected. Node C is located considering geometric restrictions. Location of nodes N and F (Fig. 3) are arbitrary because they do not affect the lateral strength (Q). Location of nodes in the stub of Fig. 4 and orientation of struts in beam are chosen so as to maximize the strength.

The strut distribution agreed with the crack pattern observed in the test for both specimens (Figs. 3 & 4). The computed tensile forces in the ties also agreed with the observed strains in the reinforcement. For example, the observed strain of the bottom beam bar of O-1 specimen was much larger than that that of

O-2 specimen as was in STM. The observed strains in the stirrups and the vertical reinforcement in the wall panel were as large as those in STM.

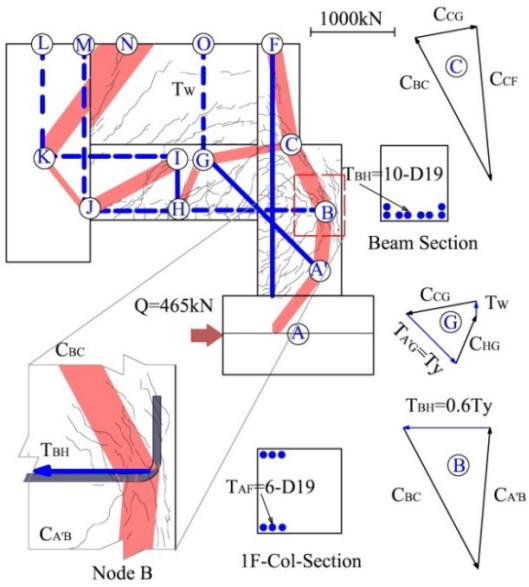

Fig.4 Strut and tie model of O-2(Opening)

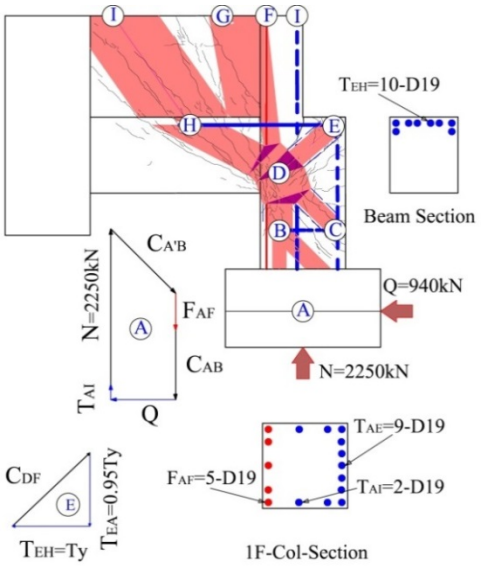

Fig.5 Strut and tie model of O-1(Closing)

Lateral load carrying capacities based on STMs (Q) also agreed with the observed strengths with errors less than 10%. Recall that the observed strengths of both specimens were less than 2/3 of the strength based on the conventional flexural analysis (Fig. 2). There are two reasons for this. A major reason is that in the conventional analysis, full depth of the first story column was considered effective. In the strut-and-tie models, node B is located at the outermost point of hooked beam bottom bars (Fig. 4) resulting in smaller distance between the compressive strut and the tensile reinforcement. This is equivalent to the reduced effective depth of the first story column. The other reason is the location of the critical section. In the conventional analysis, the critical section was assumed at the level of beam bottom face. In the STM, node B is located at the height of beam bottom reinforcement, which is equivalent to the longer shear span (= M/Q) than usual.

Figures 5 and 6 show the developed strut-and-tie models for closing direction of O-1 and O-2 specimens, respectively.

In addition to the 1st and 3rd assumptions for the opening direction, the following assumptions were made for the closing direction:

(5) The three layers of the column main bars (ACE and AI in Figs. 5 and 6) resist tension. The beam top bars also resist tension.
(6) First layer of first story column main bars yield in compression (AF in Figs. 5 and 6) as was observed in the test.
(7) Inclined bars also yield in compression (red in Fig. 6) because the observed strain was close (80%) to the yield strain.

The STM for O-2 specimen with inclined bars was developed first applying axially compressive force onto the inclined bars, which is decomposed into two components shown by red arrows in Fig. 6, and then superimposing the equivalent vertical force shown by green arrow onto the remaining system.

The strut distribution agreed well with the cracks observed in the test as shown in Figs. 5 and 6. The stresses in the reinforcement also agreed with the observation. In the tests of the both specimens, the beam top bars yielded while the first story column main bars did not yield, which was considered joint failure. In the strut-and-tie models, the beam top bars yielded while the stresses in the first story column bars were 95% and 90% of the yield strength for O-1 and O-2, respectively.

The biggest difference between the tests and the analyses was the strength. As shown in Fig. 2, the observed strength of O-2 specimen was 10% *smaller* than that O-1 specimen. As shown in Figs.5 and 6, the computed strength of O-2 specimen was 10% *larger* than that O-1 specimen.

This difference can be attributed to the contribution of the inclined bars in O-2 specimen. In the test, the inclined bars failed to transfer the compressive force to the second story and did not yield whereas in the STM they are assumed to yield in compression. It should be noted in Fig. 6 that the compressive force of the inclined bars cannot be well anchored within the first story column.

4. STRUT-AND-TIE MODELS FOR KNEE JOINT

In order to investigate the difference and the similarity between the joints in Fig. 1 and usual knee joints, STMs are constructed for a knee joint as shown in Figs. 7 and 8. The procedure and assumptions to construct STM are same as before. The reinforcement details are similar to those of the test specimens. The biggest difference is that the wall panel and the second

story column are removed.

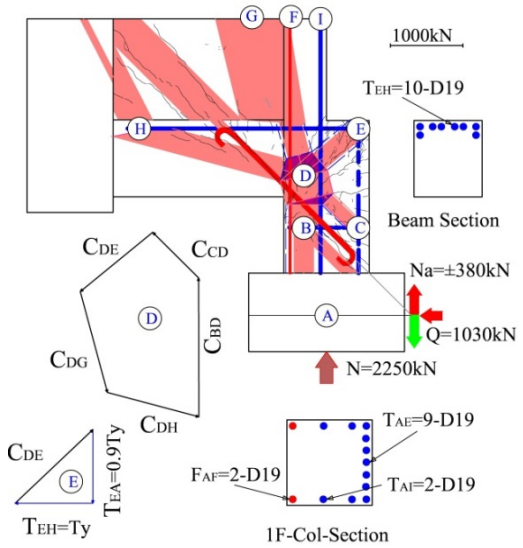

Fig.6 Strut and tie model of O-2(Closing)

In addition, virtually no axial force is applied both in opening and closing directions, except those required for equilibrium. The axial force of 2250kN that was applied in the closing direction for the test specimens cannot be applied to the knee joint, because the beam cannot resist the shear force of 2250kN.

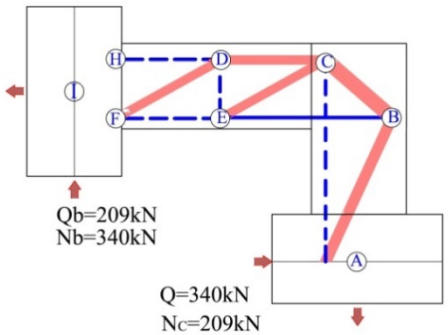

Fig.7 Strut and tie model of knee joint (Opening)

The lateral load capacity of the knee joint based on STM is much smaller than that of the test specimens in both opening and closing directions. The capacity of the knee joint was governed by beam flexural capacity. Beam stirrups (in STM) were enough to resist beam shear force.

The difference of the capacities in the opening load is attributable to the difference of the location of node C. Note that node C in Fig. 3 is located to the right compared with that in Fig. 7. This leads to smaller inclination of strut BC resulting in larger compressive force in strut AB and larger tensile force in tie AC. Also note that the inclination of strut CF in Fig. 3 is opposite to that of strut AB, indicating that the sign of the shear force in the second story column is opposite to that of the first story column. The cracks observed in the test also support this tendency. This negative shear force is compensated by strut KN in the shear wall.

In the closing direction, the orientation of struts DG and DH in Fig. 5 is different from that of DG and DH in Fig. 8, which was caused by the large axial force in the test specimen. In Fig. 5 most of the shear force is transferred to the shear wall panel, which led to larger capacity of the test specimen than the usual knee joint.

On the other hand, there are important similarities between the test specimens and the knee joint. In the opening load, node B is located inside the hook of the beam bars, limiting the capacity of the first story column as discussed later. In the closing load, node E is resisted by the tensile forces of the column and beam bars, which indicates that the beam top bars in a frame shown in Fig. 1a should be designed according to the provisions for knee joint making the tail length long enough.

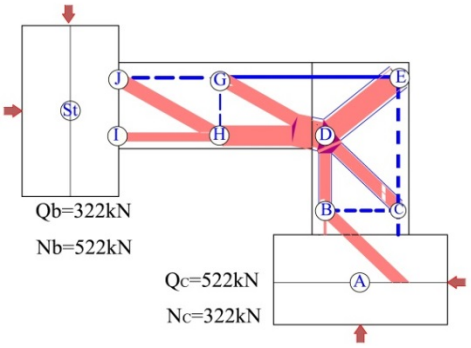

Fig.8 Strut and tie model of knee joint (Closing)

5. STM FOR A PROTOTYPE FRAME

Figure 9 shows a strut-and-tie model for a transverse frame of full-scale structure. The building structure is assumed to be 5-story single bay apartment building with span length of 12m and the transvers frames spaced 12m along the building length. This figure represents overall flow of forces in the frame. Ties CD and BG are located close to each other which means that some shear reinforcing is required in the beam near the joint. On the other hand, tie AF near the mid-span, represents stirrups of a big portion of beam-span length which means smaller amount of stirrups are required in mid-span of the beam.

The diagrams at the bottom of Fig. 9 show the axial-force, shear-force, and bending moment of the boundary beam computed based on the STM. In the axial force diagram, graph above the horizontal axis represents compressive force. In the opening joint (right), the beam is subjected to tensile axial force and led to a smaller flexural capacity of beam whereas in the closing joint (left) it resists compressive axial force with lager bending moment capacity as shown in Fig. 9. The shear force in the opening joint (right) is resisted by stirrups, while the shear force in the closing joint (left) is resisted by concrete strut. The bending moment diagram indicates that the beam bottom reinforcement needs to be provided all along the span whereas the top reinforcement needs not.

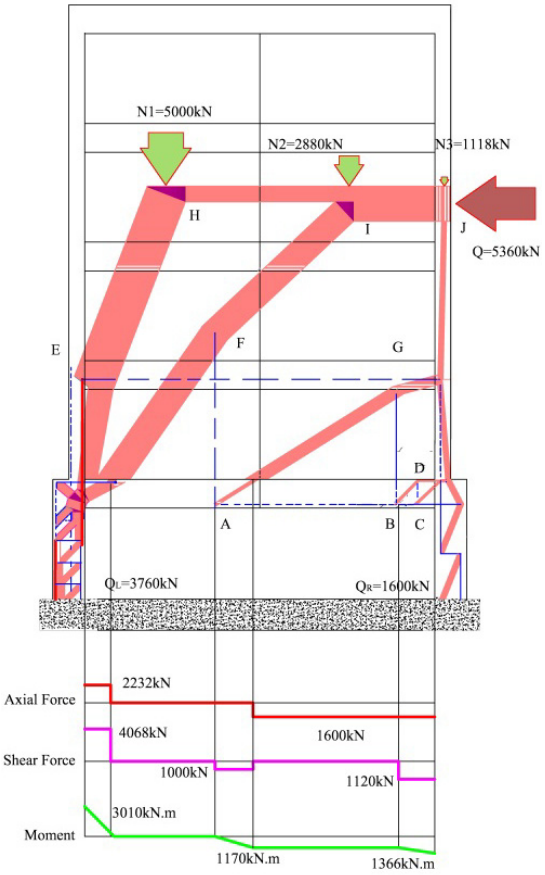

Fig.9 Strut and tie model of a 5 story building frame

6. DESIGN EQUATIONS

Following the results of strut and tie analysis, simplified design equations are proposed in this research.

The ultimate lateral strength of the beam-column joint Q_u is the smaller of the first story column strength Q_c and that of the joint strength Q_j.

$$Q_u = \min[Q_c, Q_j] \quad (2)$$

The objective of this equation is not to prohibit the joint failure: because failure in the joint exhibited large ductility, joint failure is acceptable.

The critical sections of the column failure and joint failure are assumed as shown by broken lines in Fig. 10 based on the strut and tie model. The strength of the first story column Q_c is calculated by the following equation.

$$Q_c = \frac{M_{c1}}{L + l_c} \quad (3)$$

where,

M_{c1}: the moment capacity at the top of the column

L: the length between the point of contra flexure and top of the first story

l_c: the distance between the top of the first story column and the centroid of the beam bottom bars

In eq. (3), $(L + l_c)$ is the shear span length whereas L is usually called the shear span length. In opening direction, the critical section is l_c above the top of the first story column as shown in Fig. 10(a). In closing direction, the centroid of the rectangle which is connected to two struts (BD and CD in Fig. 10c) in the first story column is on the critical section. The location of this point is close to the centroid of beam bottom reinforcements in usual beams. In fact, the distance l_c is from 56 mm to 61 mm in this research and the centroid of the rectangle is 50 mm above the top of the first story column.

The effective depth of the first story column is smaller than the actual depth of the first story column because concrete outside the anchorage of the beam bottom reinforcement is not effective to compressive force as shown in Fig. 10(a). In this research, 420 mm is used as the effective depth. To consider the effective depth in the moment capacity of the first story column, the following equation is used.

$$M_{c1} = \frac{D_{eff}}{D_{c1}} \cdot M_0 - N \cdot \frac{D_{c1} - D_{eff}}{2} \quad (4)$$

where,

D_{eff}: effective depth of the first story column

D_{c1}: actual depth of the first story column

M_0: the moment capacity of the column considering the full section

The joint strength Q_j is calculated by the following equations.

$$Q_j = \frac{M_j}{L + D_b/2} \quad (5)$$

$$M_j = M_{c2} + M_b \quad (6)$$

$$M_b = \begin{cases} M_{b0} - 0.4 Q_j D_b & \text{for opening} \\ M_{b0} & \text{for closing} \end{cases} \quad (7)$$

where,

M_{c2}: the moment capacity of second story column around the center of the first story column

M_b: the moment capacity of beam

M_{b0}: the beam moment without axial force

D_b: beam depth

Equation (7) and its application are explained in the following paragraph.

The moment capacity of the joint is defined around the joint center (white circle) as shown in Figs. 10b and d. In these figures, forces acting on the critical sections are also shown. Contributions of vertical forces acting on the critical section are computed as the moment capacity of the second story column. Similarly, contributions of horizontal forces acting on the critical section are computed as the moment capacity of the beam. The beam moment is computed as:

$$M_b = C_h(\alpha.D_b) + T_h(d - \frac{D_b}{2}) \quad (8)$$

$$M_b = M_{b0} - \alpha.D_b.Q_j \quad (9)$$

The term $(\alpha.D_b)$ represents vertical distance of C_h from the beam centerline (or white circle) and in this study it is assumed to be $0.4D_b$ (Fig. 10b). The second term in eq. (9)/eq. (7) represents contribution of beam

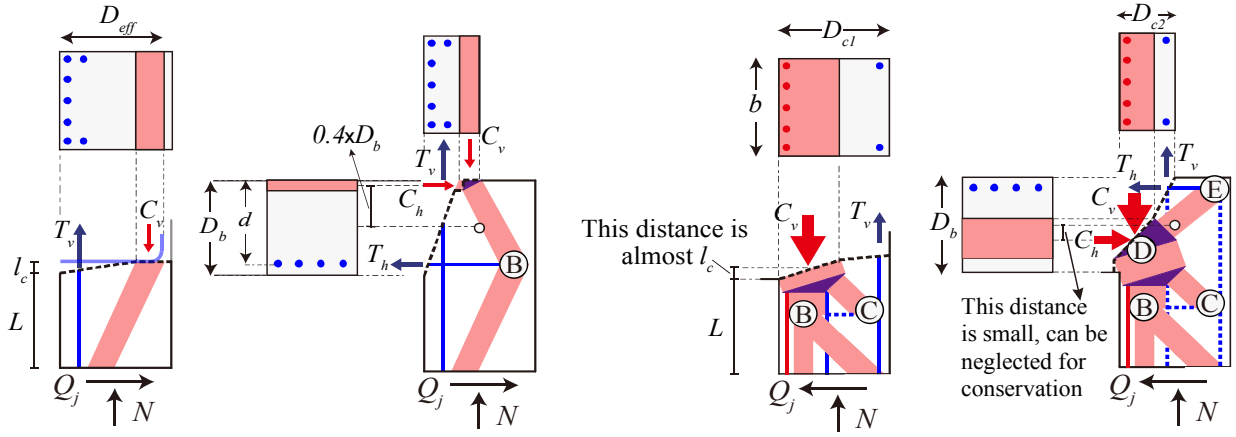

(a) Column (Open) (b) Joint (Open) (c) Column (Close) (d) Joint (Close)

Fig. 10 Critical sections

axial force which is equal to $-Q_j$ (tensile) and $+Q_j$ (Compressive) for opening and closing direction, respectively. In closing direction, contribution of beam axial force is negligible because the location of this force is near the centerline of the beam as shown in Fig. 10(d). In this calculation, iteration method is needed because the joint strength Q_j is not known yet, but Q_c can be used in the first iteration to converge soon.

Recalling back to Fig. 9, it is difficult to know the axial forces in the columns and the beam. Variables like M_0, axial force in the columns, and Q_j are correlated to each other. Again, iteration is needed to get an optimum solution.

Figure 11 shows the comparison between observed and calculated strength. Proposed design equations evaluate the strengths of the specimens appropriately. On the other hand, design equations cannot predict failure modes in the cases of O-1 (opening) and O-1t (closing). In these cases, the strengths of the joint and the column are close to each other. Although design equation cannot distinguish the failure modes in such case, it can estimate the strength.

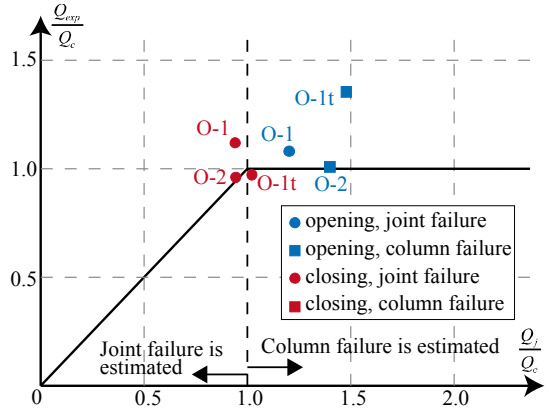

Fig. 11 Estimated and observed strengths

Lateral strength of a single-bay frame e.g. Fig. 9, can be considered as summation of the shear force in right and left columns. Because, deformation of both (left and right) columns at their maximum strength is almost equal to each other (Fig. 2).

7. CONCLUSIONS

(1) Strut-and-tie models agreed with the observed crack patterns and the measured strains.

(2) Comparison between strut-and-tie models of usual knee joint and that of the specimens shows that the flow of forces and corresponding strength of usual knee joints are very different from that of the beam-column joint with shear wall in the upper stories.

(3) Embedment length of beam bars should be regarded as effective depth of the first story column for opening load.

(4) Strength relative to the joint failure can be approximated to the sum of the strength of beam and that of the second story column.

REFERENCES

[1] Shiohara, H., Y. W. Shin (2006), "Analysis of Reinforced Concrete Knee Joints Based on Quadruple Flexural Resistance," *Proceedings of the 8th U.S. national Conference on Earthquake Engineering*, San Francisco, California, USA, P No. 1173

[2] Iizuka, M., K. Araki, Y. Miura, K. Yabuzaki, and H. Shiohara (2007) "Study of Exterior Column-Pile-Foundation Beam Joint (Part-1 Proposal of Critical Sections)," *Summaries of Technical Papers of Annual Meeting*, AIJ, Vol. C-2, pp. 359-360. (in Japanese)

[3] G. Kotani, S. Takahashi, H. Fukuyama, and T. Ichinose (2011), "Strength and Failure Mode of RC Beam-Column Joint in Soft-First Story where First-Story Column Extended Outside," *Proceedings of the Japan Concrete Institute*, Vol. 33, No. 2, pp.313-318. (in Japanese)

[4] Hognestad, E., N. W. Hanson, and D. McHenry (1955), "Concrete stress distribution in ultimate strength design," *ACI*, Vol. 27, No. 4, pp.455-479